Simulation of Meshing Rack and Pinion for Steering Systems*1

D. MAEDA K. YAMANAKA

Rack and pinion systems used for steering systems present several unique points. The first is that the racks used are generally round, and are supported without restraint against rack rotation. Second, the rack is supported by a spring that is pressed against the pinion, and under no or light load, the front and back tooth surfaces mesh. Because of this unique structure, conventional meshing simulation, which determines the distributed load on tooth surfaces, has not been applied. The influence of distributed load on performance is significant and should be evaluated at the design stage. This influence was dealt with by adding the equivalent error of tooth surfaces due to the motion of the rack and the distributed load due to the meshing on the back tooth surface to the conventional tooth deformation formula used for meshing simulation. As a result of the analysis, it was confirmed that the displacement caused by the rack behavior and the meshing of both tooth surfaces, which is unique structure of steering rack and pinion systems, could be reproduced. Verification was also performed using actual equipment.

***Key Words**: steering system, rack and pinion, meshing simulation, tooth deformation formula*

1. Introduction

Automotive steering systems are considered to be parts critical for safety and require a high level of reliability. They are also being required to provide higher output while being more compact in order to support electrification and carbon neutrality. Until now, transmission system components have been designed by conducting theoretical estimations of rack swing torque and physical property modeling of steering performance[1), 2)]. However, gear design has not been performed by taking tooth deformation and the resulting distributed load to tooth surfaces into account. Because the load distributed to the surfaces of meshed teeth exerts a significant impact on performance, it is possible to enhance product quality by taking this into account during the design process. This paper presents the results of our efforts to improve upon the conventional meshing analysis method[3)] that uses a tooth deformation formula by enabling the displacement caused by rack behavior and the meshing of both tooth surfaces, which are unique characteristics of steering rack and pinion systems, to be taken into account. Also presented are the results of verifications performed using actual equipment.

2. Characteristics of Steering Rack and Pinion Systems

The steering rack and pinion structure shown in **Fig. 1** has the following three characteristics. Firstly, the racks used are generally round. Although the support structure does not restrain rack rotation, the meshing of the pinion and rack does restrain rack rotation. Secondly, the pinion and rack are not perpendicular to each other and cross at an angle due to mounting conditions on the vehicle. This causes slippage in the tooth trace direction, causing frictional force to generate torque that rotates the rack. Thirdly, the rack is supported by a spring pressed against the pinion via a guide in order to reduce noise caused by backlash. As a result, both the front and back tooth surfaces mesh under no or light load. When the load is high, the spring is pushed, causing the clearance on the guide back surface to disappear and only the front tooth surface to mesh.

*1 This paper was created based on Transactions of the 2021 JSME Mechanical Engineering Congress (No. 21-1, September 2021, p. 754-758) and by adding actual equipment verification results.

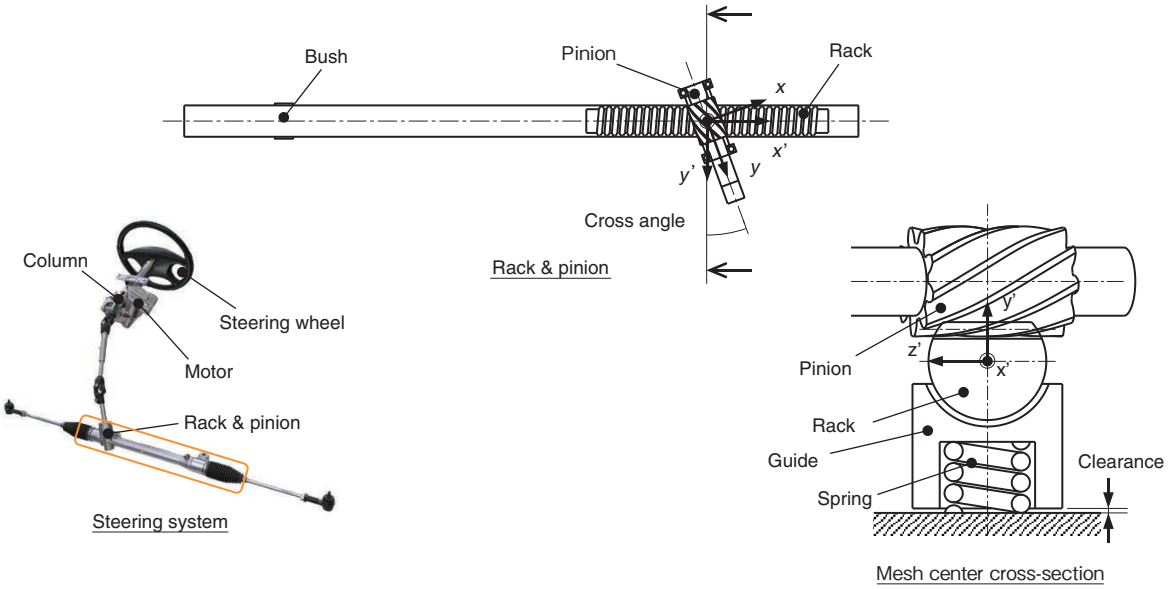

Fig. 1 Structure of steering rack and pinion (C-EPS)

3. Meshing Analysis

We have succeeded in improving the conventional meshing analysis method by using Tooth Deformation Formula (1) capable of accounting for the characteristics described in the previous section.

$$\int_0^{L(t)} K_b(x,\xi)p(\xi)d\xi + K_c(x)p(x) = \delta_0(x) = \{\Delta - e(x)\}\cos\beta_g \quad (1)$$

Formula legend

t	: Constant representing the relative rotation angle position of the gear and thus the position of the contact line on the tooth surface
$L(t)$	: Length of the contact line at t
x	: Measurement coordinate for deformation on the contact line
ξ	: Coordinate for the effective load center on the contact line
$K_b(x, \xi)$	: Compliance of tooth deflection for a pair of meshed teeth
$K_c(x)$	: Compliance of elastic contact for a pair of meshed teeth
$p(\xi)$	: Distributed load
$\delta_0(x)$	: Tooth deformation at point x
Δ	: A value obtained by converting the lag angle of driven gear with respect to the driving gear into a distance on the line of action (perpendicular to the axis)
$e(x)$	: Equivalent error at point x of the pair of meshed teeth (perpendicular to the axis)
β_g	: Base helix angle

The following three improvements have been made. First, a FEM model is used for calculating tooth compliance. Although only the deformation of the front surface where load is applied has been used conventionally, in order to take into account the meshing of both tooth surfaces, the deformation of the back surface where no load is applied has also been used as shown in **Fig. 2**. Second, the tooth deformation formula is an integral equation that includes the contact line on the back surface. As shown in **Fig. 3**, the front and back contact lines can be obtained geometrically. Third, an equivalent error is used. Changes in the rack tooth surface due to motion in the rack axis direction, guide axis direction, and direction around the rack axis shown in **Fig. 4** are included in the equivalent error. Also, the Lundberg equation was used for the influence function for approach due to contact.

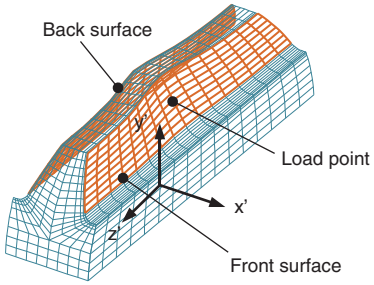

Fig. 2 FEM model for calculating tooth compliance

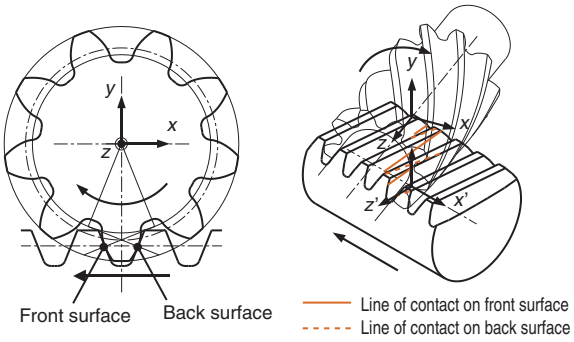

Fig. 3 Contact lines on front and back tooth surfaces

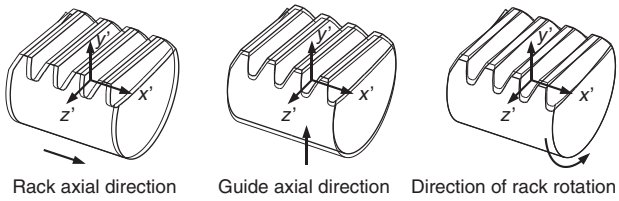

Fig. 4 Displacement of tooth surface due to the motion of rack

4. Analysis Results

Meshing analysis was conducted using the specifications of rack and pinion that imitate steering shown in **Table 1**. **Figure 5** shows analysis results for contact pressure distribution on the pinion tooth surface when the rack load is changed from 0 N to 4 000 N. These results are for specification No. 1 which has a pinion helix angle of 25 degrees. Here, σ_{Hmax} represents the maximum contact pressure, while θ_{ave} represents the average rack rotation angle. When the rack load is low, the spring load causes both the front and back tooth surfaces to mesh. The cross angle causes slippage of the tooth surface, which in turn causes frictional torque to generate torque that rotates the rack, resulting in slightly stronger uneven contact in the negative direction of the tooth width. As the rack load increases, the tooth surface load and rack helix angle generate torque in the opposite direction, reducing the rack rotation angle and alleviating uneven contact. When the rack load exceeds 2 000 N, the spring is pushed and only the front tooth surface meshes. Steering rack and pinion systems have several pinion teeth, and because no modifications were made to the tooth profile direction, high loads cause high contact surface pressure to be generated at the root of pinion teeth.

Next, **Fig. 6** shows the contact pressure distribution for specification No. 2, which has a pinion helix angle of 35 degrees. When rack load is low, the cross angle causes slightly stronger uneven contact in the negative direction of the tooth width in the same manner as specification No. 1. As rack load increases, the torque that rotates the rack in the opposite direction increases more than in specification No. 1 because the rack helix angle of specification No. 2 is larger. As a result, strong contact occurs in the positive direction of the tooth width, causing uneven contact and resulting in the contact pressure increasing from 2 524 MPa of specification No. 1 to 2 953 MPa. In this manner, we succeeded in improving the meshing analysis by enabling the characteristics of the steering rack and pinion system, such as meshing on both tooth surfaces and uneven contact due to rack rotation, to be taken into account.

Table 1 Specifications of rack and pinion that imitate steering

	No. 1		No. 2	
	Pinion	Rack	Pinion	Rack
Module	2			
Pressure angle	20 deg			
Helix angle	25 deg (Left)	5 deg (Right)	35 deg (Left)	15 deg (Right)
Number of teeth	9	–	9	–
Profile shift coefficient	0.3	–	0.1	–
Pitch circle diameter	19.861mm	–	21.974mm	–
Base circle diameter	18.430mm	–	20.081mm	–
Pitch line height	–	7mm	–	7mm
Addendum	2.2mm	1.6mm	1.8mm	1.6mm
Dedendum	1.5mm	2.1mm	1.9mm	2.1mm
Rack shaft diameter	–	26mm	–	26mm
Center distance	17.530mm		18.187mm	
Cross angle	20 deg			
Spring load	500 N			
Clearance	0.05mm			

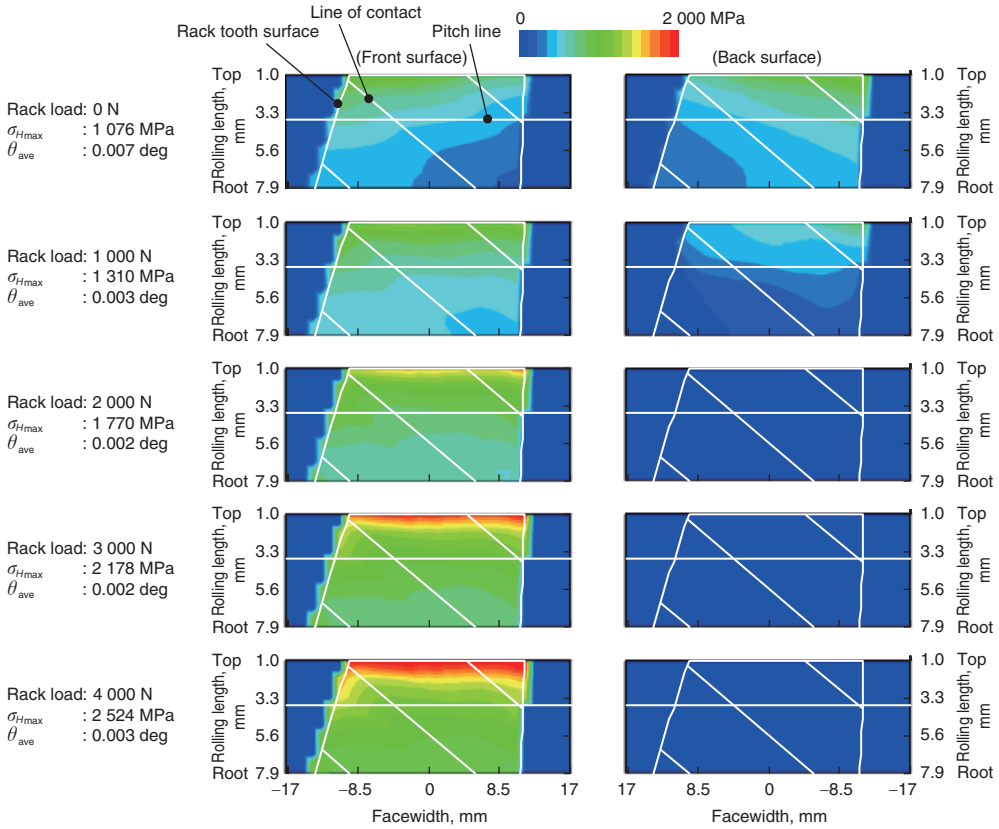

Fig. 5 Distribution of contact pressure on pinion tooth surface (No. 1)

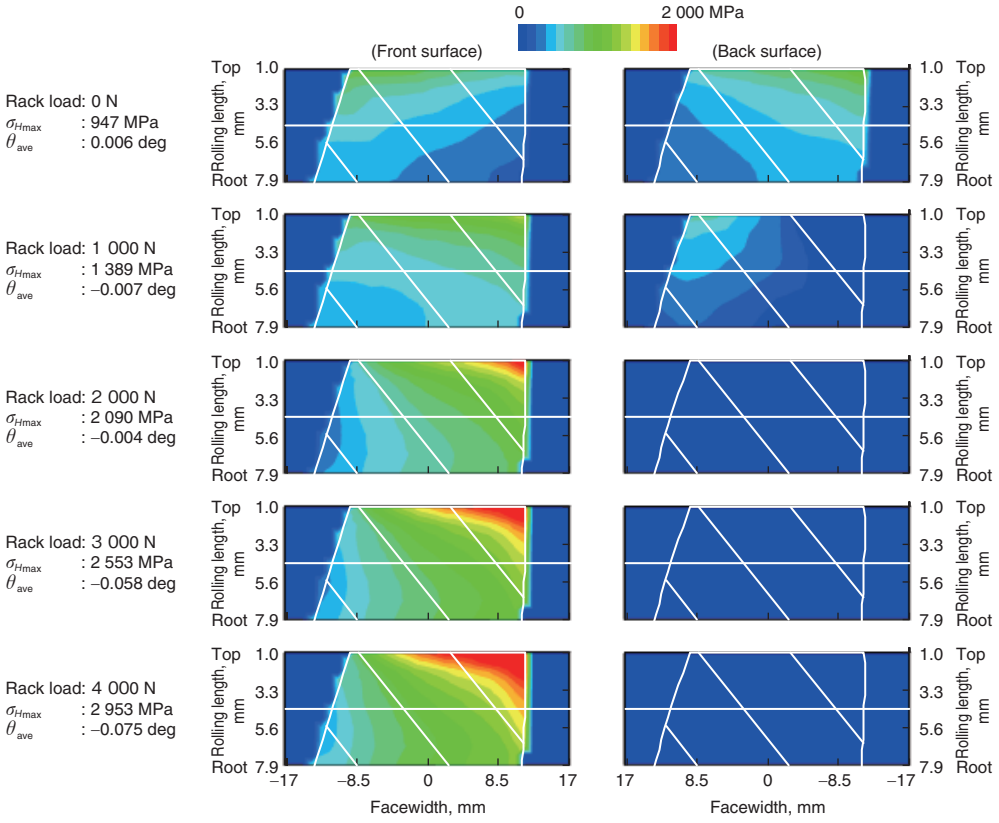

Fig. 6 Distribution of contact pressure on pinion tooth surface (No. 2)

5. Actual Equipment Verification

We manufactured the samples shown in **Table 1** and verified the following two items to determine whether the meshing analysis of the improved steering rack and pinion system can be used to achieve a design that meets performance requirements.

5. 1 Rack Sliding Load

Reverse sliding load fluctuation, which is the rack sliding load when the pinion is unloaded as shown in **Fig. 7**, is used as an indicator for steering feeling performance. Because this is caused by tooth surface friction generated by the spring load presses the guide, we verified whether it can be reproduced by integrating friction force with the rack axial force. Each sample was manufactured by grinding the tooth surfaces, after which assessment was performed using a device capable of adjusting the cross angle with an accuracy of 0.01 deg or less. The coefficient of friction used for the tooth surface during the analysis was 0.08. **Figures 8** and **9** show the actual equipment and analysis results for specification No. 1 in **Table 1** when cross angle misalignment occurs. **Figure 8** shows that rack sliding load fluctuation is low when the cross angle misalignment is 0, while (b) in **Fig. 9**, in which the horizontal axis represents the pinion rotation angle, also confirms that fluctuation is low. As shown in **Fig. 8**, fluctuation increases as cross angle misalignment increases. As shown by (a) and (c) of **Fig. 9**, rack sliding load fluctuation occurs during the meshing cycle, and the waveform and phase of the generated fluctuation can be reproduced. **Figure 10** shows the analysis results for the distribution of load on the pinion tooth surface under the same conditions. When the crossing angle misalignment is negative, uneven contact between the front and back surfaces tends to increase while the overlap ratio decreases, resulting in increased fluctuation. When the crossing angle misalignment is positive, uneven contact tends to be greater on the

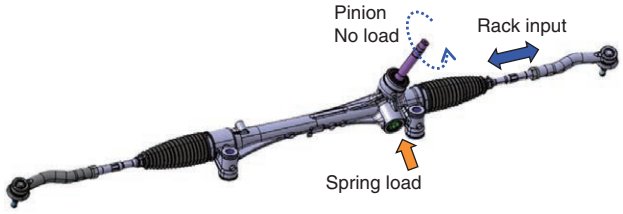

Fig. 7 Rack sliding load

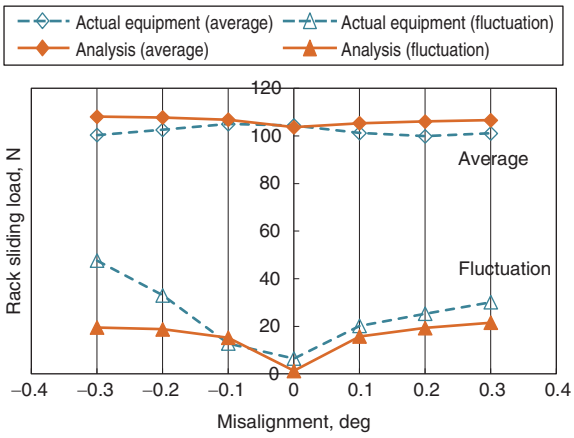

Fig. 8 Rack sliding load

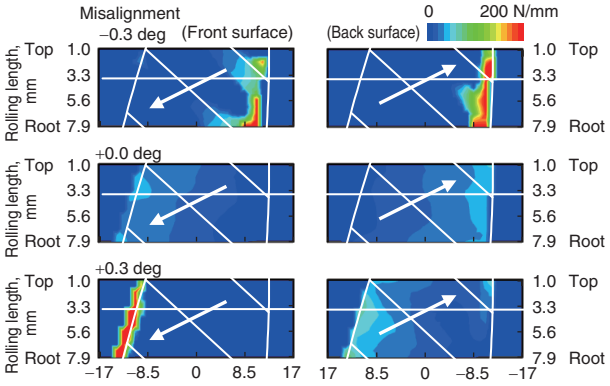

Fig. 10 Distribution of load on pinion tooth surface

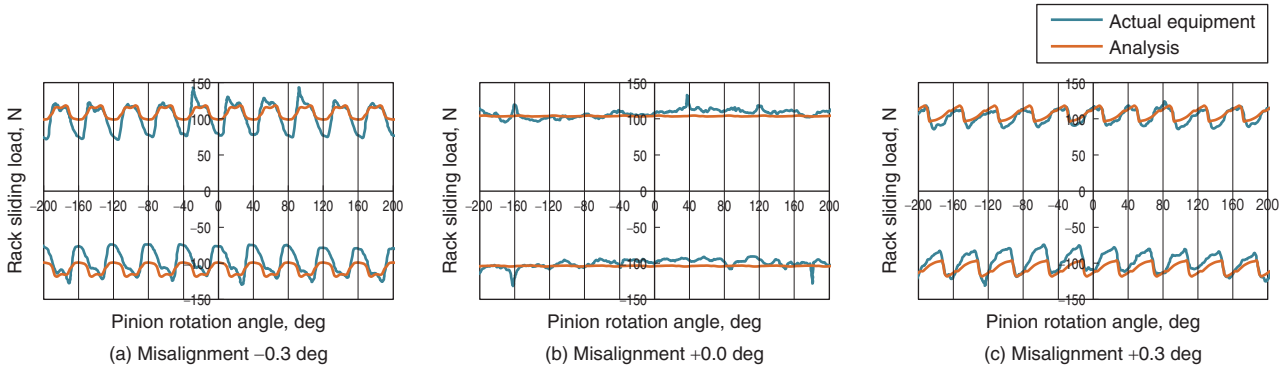

Fig. 9 Rack sliding load

front side, however, tooth contact on the back side will be slightly wider. In this manner, we were able to successfully verify the validity of the analysis model used to calculate the rack sliding load from frictional force generated by tooth surface slippage.

5. 2 Tooth Surface Wear

In the endurance test for assessing reliability, a load is applied to the rack side while input from the pinion is used to perform reciprocal operation. During the endurance test, the tooth surface suffered the adhesive wear shown in **Fig. 11**. Formula (2) shows a wear model that uses the surface pressure and sliding ratio necessary to reproduce this wear.

$$\delta = CP^2\sigma N \quad (2)$$

Formula legend
δ : Wear depth
C : Specific wear rate
P : Surface pressure
σ : Sliding ratio
N : No. of endurance cycles

The tooth surface, which changes from moment to moment due to wear, is expressed as an equivalent error in Formula (1) and is reproduced by repeating the analysis. Based on the amount of surface wear on the teeth of the actual equipment, 0.265×10^{-7} (mm/(GPa)^2) was used for the pinion specific wear rate, while 0.214×10^{-7} (mm/(GPa)^2) was used for the rack specific wear rate. **Figure 12** shows the analysis results for tooth surface wear and surface pressure distribution at a rack load of 8 000 N and 60 000 cycles for specification No. 1 in **Table 1**. During the early stages of analysis, it can be confirmed that the pinion root suffers wear in areas where the surface pressure is high. This wear then causes the surface pressure to decrease. Moreover, repeated analysis causes the surface pressure distribution to change

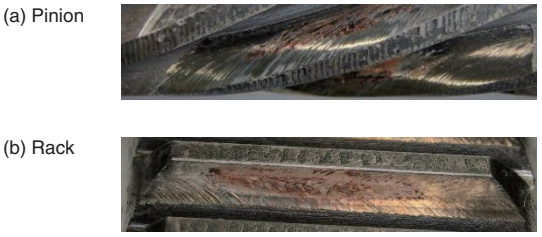

Fig. 11 Tooth surface after endurance test

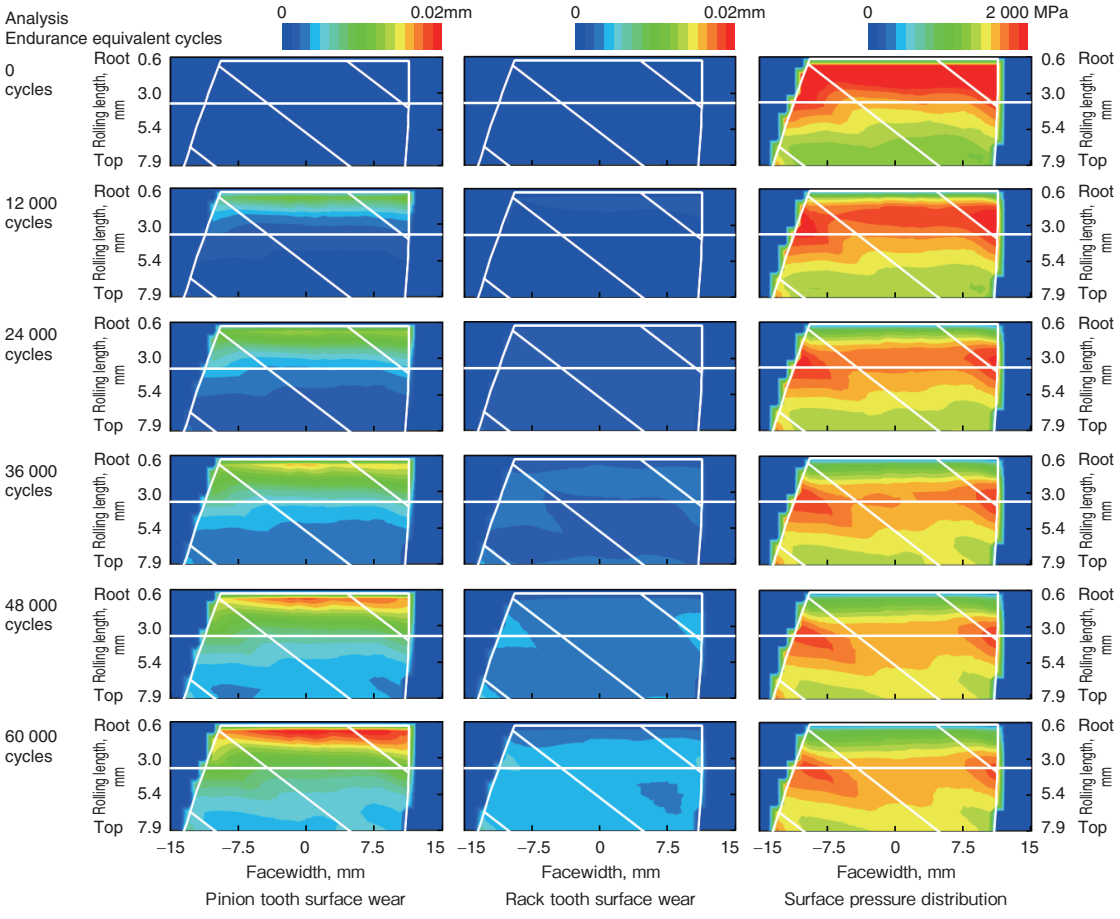

Fig. 12 Analysis to calculate tooth surface wear

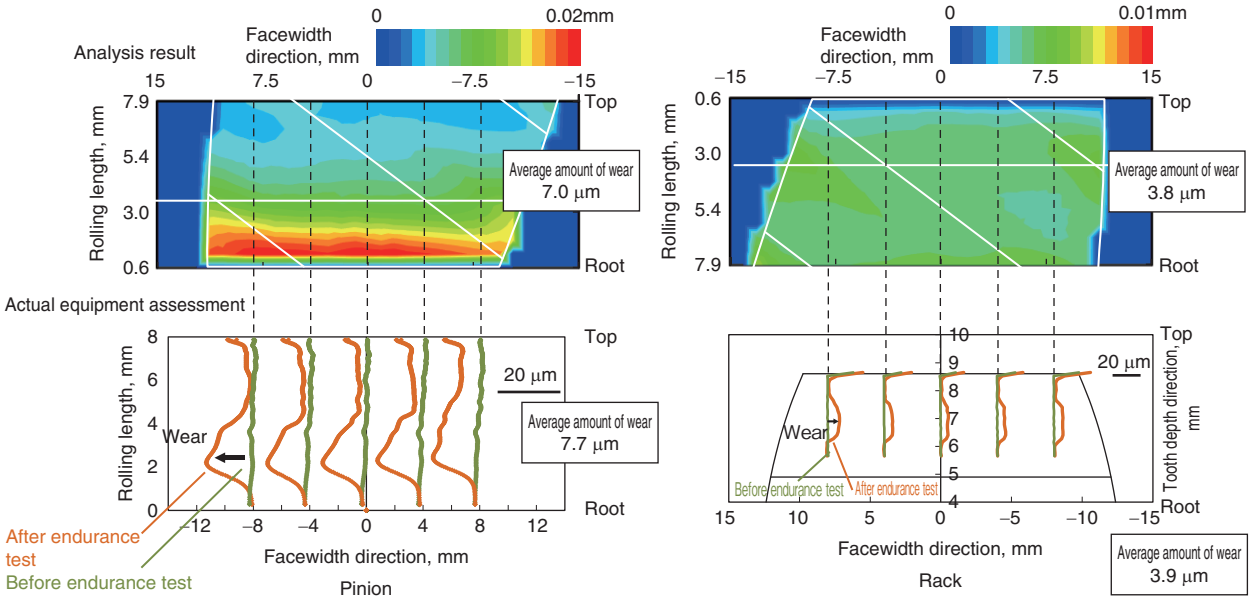

Fig. 13 Analysis and verification result

gradually. **Figure 13** shows the amount of pinion and rack wear suffered during analysis, as well as measurement results for the tooth surfaces on the actual equipment. After undergoing induction hardening, grinding was performed on the tooth surfaces of the samples, which were then assessed using the same amount of lubricant as the mass-produced product. The pinion root showed a large amount of wear, similar with the wear distribution seen on the actual equipment, verifying the validity of the analysis model in estimating tooth surface wear.

6. Conclusion

We have succeeded in improving upon the conventional meshing analysis method that uses a tooth deformation formula by taking into account the unique characteristics of steering rack and pinion systems, namely, rack rotation and the meshing of both tooth surfaces. Using actual equipment, we verified the analysis performed on rack sliding load and tooth surface wear, and confirmed that the distributed load on the tooth surfaces of meshing gears influences performance. We were also able to confirm that this analysis can be used for design that takes this influence into account. In the future, we will contribute to further improvements in product quality by using our developed meshing analysis method.

* C-EPS is a registered trademark of JTEKT Corporation.

References

1) T. KOBAYASHI, H. SHIBATA: Estimation of Rack Swing Torque for Rack and Pinion Steering Gear, JTEKT ENGINEERING JOURNAL, No. 1006E (2009) 23-30.
2) S. NAKANO, T. TAMURA, S. KIMURA, A. KUBO: Strategy for Transfer Elemental Designing, Employing Physical Characteristic Modeling of Steering Maneuver. (Second Report: Improvement of the Vehicle Cornering Characteristics during Slight Steering Operation), Transactions of the JSME Series C, 79, 806 (2013).
3) A. KUBO, K. UMEZAWA: On the Power Transmitting Characteristics of Helical Gears with Manufacturing and Alignment Errors, (1st Report, Fundamental Consideration), Transactions of the JSME, 43, 371 (1977) (in Japanese).


D. MAEDA* K. YAMANAKA*

* *Systems Innovation R&D Dept., Research & Development Division*